

Pillar[10]arene-based host–guest complexation promoted self-assembly: from nanoparticles to uniform giant vesicles

Jie Yang, * Zhengtao Li, Li Shao and Guocan Yu*

Department of Chemistry, Zhejiang University, Hangzhou 310027, P. R. China;

Email: jieyang@zju.edu.cn; guocanyu@zju.edu.cn

Electronic Supplementary Information (11 pages)

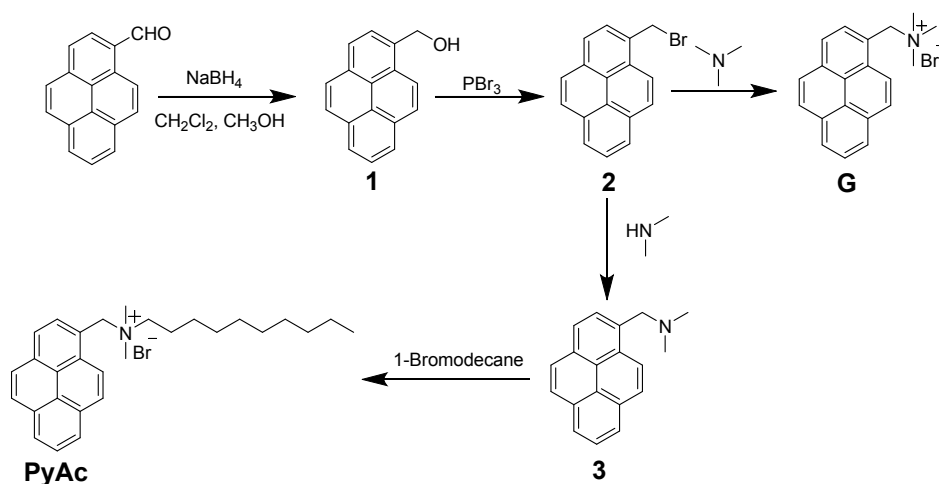
1. *Materials and methods*
2. *Syntheses of compounds **G** and **PyAC***
3. *2D NOESY spectra of **WP10**⊃**G***
4. *Isothermal titration calorimetry (ITC) experiment*
5. *Critical aggregation concentration (CAC) determination of **PyAC** and **WP10**⊃**PyAC***
6. *DLS data of **WP10**⊃**PyAC***
7. *TEM images of **G** and **WP10**⊃**G***
8. *References*

1. Materials and methods

All reagents were commercially available and used as supplied without further purification. Solvents were either employed as purchased or dried according to procedures described in the literature. Compound **1**, **2**, **3** and water-soluble pillar[10]arene (**WP10**) were synthesized according to literature procedures.^{S1,S2} NMR spectra were collected on either a Bruker Avance DMX-400 spectrometer or a Bruker Avance DMX-500 spectrometer with internal standard TMS. UV-vis spectra were taken on a Shimadzu UV-2550 UV-vis spectrophotometer. The fluorescence experiments were conducted on a RF-5301 spectrofluorophotometer (Shimadzu Corporation, Japan). Transmission electron microscopy (TEM) investigation was carried out on a JEM-1200EX instrument. The critical aggregation concentration (CAC) values of **G** and **WP10**⊃**G** were determined on a DDS-307 instrument.

2. Syntheses of compounds **G** and **PyAc**

Scheme S1. Synthetic route to **G** and **PyAc**.



Synthesis of **G**: Compound **2** (1.48 g, 5.00 mmol) and trimethylamine (33% in methanol, 5.40 mL, 20.0 mmol) were added to methanol (50 mL). The solution was refluxed overnight. Then the solvent was removed by evaporation, deionized water (20 mL) was added. After filtration, a clear solution was got. Then the water was removed by evaporation to obtain **G** as a yellow solid (1.69 g, 95%), m.p. 148.6–149.3 °C. The ^1H NMR spectrum of **G** is shown in Fig. S1. ^1H NMR (400 MHz, D_2O , 293 K) δ (ppm): 8.14 (d, $J = 8$ Hz, 1H), 8.06 (d, $J = 8$ Hz, 1H), 8.00 (d, $J = 8$ Hz, 1H), 7.90 (d, $J = 8$ Hz, 1H), 7.74 (d, $J = 8$ Hz, 1H), 7.66 (d, $J = 8$ Hz, 2H), 7.62 (d, $J = 8$ Hz, 1H), 7.52 (d, $J = 8$ Hz, 1H), 4.64 (s, 2H), 2.91 (s, 9H). The ^{13}C NMR spectrum of **2** is shown in Fig. S2. ^{13}C NMR (125 MHz, $\text{DMSO}-d_6$, 293 K) δ (ppm): 132.37, 132.26, 131.53, 130.61, 129.90, 128.87, 126.72, 125.95, 124.14, 123.47, 121.86, 64.15, 52.05. LRESIMS is shown in Fig. S3: m/z 274.2 $[\text{M} - \text{Br}]^+$. HRESIMS: m/z calcd for $[\text{M} - \text{Br}]^+$ $\text{C}_{20}\text{H}_{20}\text{N}$, 274.1596; found 274.1610; error 5 ppm.

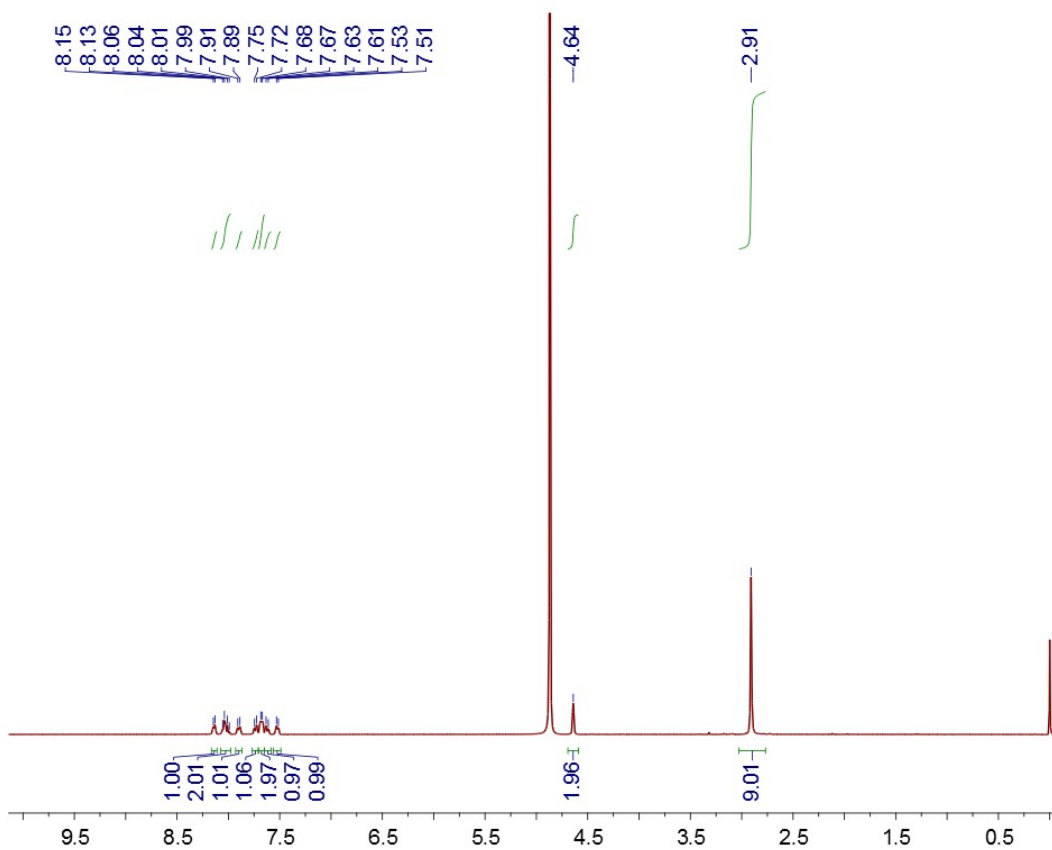


Fig. S1. ^1H NMR spectrum (400 MHz, D_2O , 293 K) of **G**.

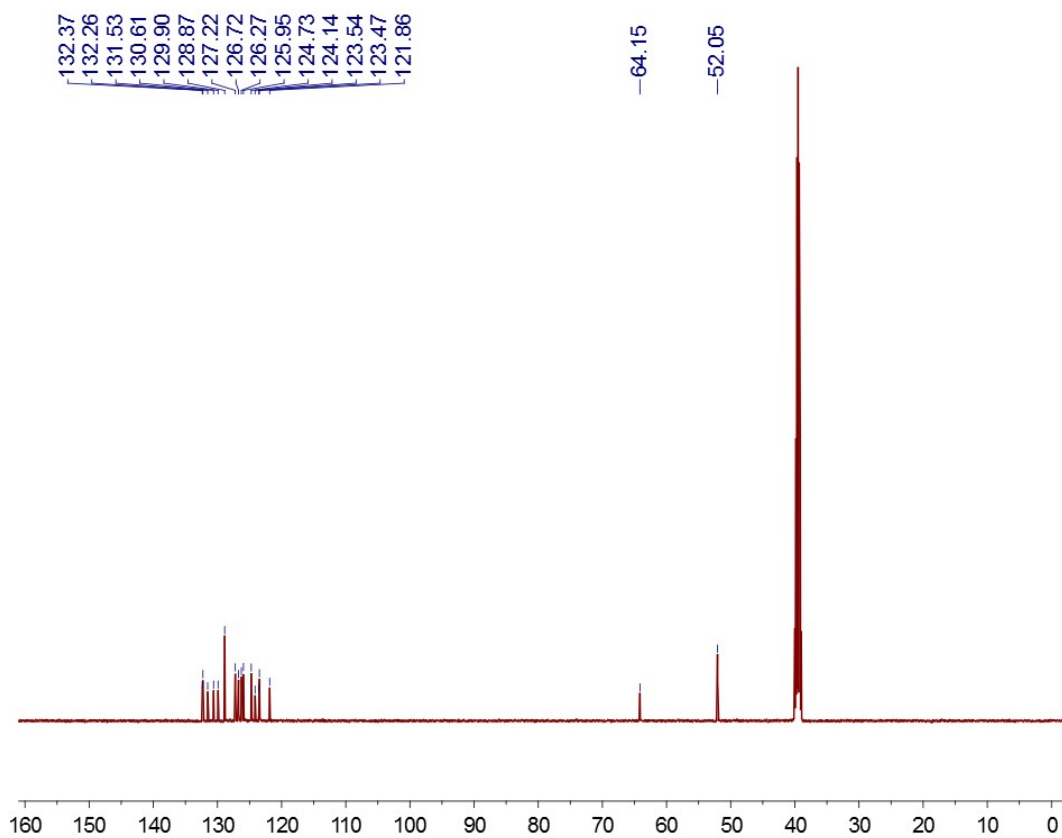


Fig. S2. ^{13}C NMR spectrum (125 MHz, $\text{DMSO}-d_6$, 293 K) of **G**.

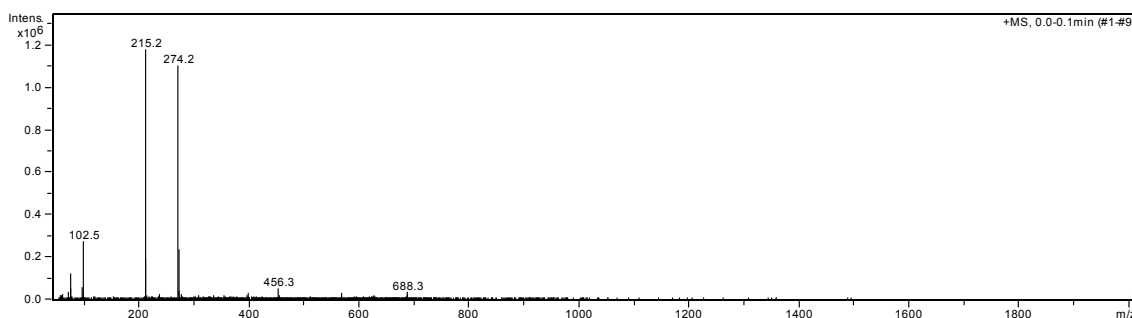


Fig. S3. Electrospray ionization mass spectrum of **G**. Assignment of the main peak: m/z 274.2 $[M - Br]^+$ (100%).

Synthesis of **PyAC**: Compound **3** (2.59 g, 10.0 mmol) and 1-bromodecane (4.42 g, 20.0 mmol) were added to CH_3CN (100 mL). The solution was refluxed overnight. After filtration, the filtrate was washed by CH_3CN (3×50 mL). The product was dried in vacuum oven to give **PyAC** as a yellow solid (4.43 g, 92%), m.p. 114.3-114.8 °C. The 1H NMR spectrum of **PyAC** is shown in Fig. S4. 1H NMR (400 MHz, $DMSO-d_6$, 293 K) δ (ppm): 8.78 (d, $J = 10$ Hz, 1H), 8.44 (m, 4H), 8.32 (m, 3H), 8.19 (t, $J = 10$ Hz, 1H), 5.35 (s, 2H), 3.51 (m, 2H), 3.06 (s, 6H), 1.84 (s, 2H), 1.27 (m, 14H), 0.86 (t, $J = 10$ Hz, 3H). The ^{13}C NMR spectrum of **PyAC** is shown in Fig. S5. ^{13}C NMR (125 MHz, $DMSO-d_6$, 293 K) δ (ppm): 132.36, 132.26, 131.65, 130.62, 129.88, 128.90, 128.86, 127.21, 126.73, 126.31, 125.97, 124.74, 124.14, 123.53, 123.39, 121.60, 63.98, 49.05, 31.24, 28.46, 25.90, 22.06, 21.90, 13.94. LRESIMS is shown in Fig. S6: m/z 400.3 $[M - Br]^+$. HRESIMS: m/z calcd for $[M - Br]^+$ $C_{29}H_{38}N$, 400.3004; found 400.3000; error -1 ppm.

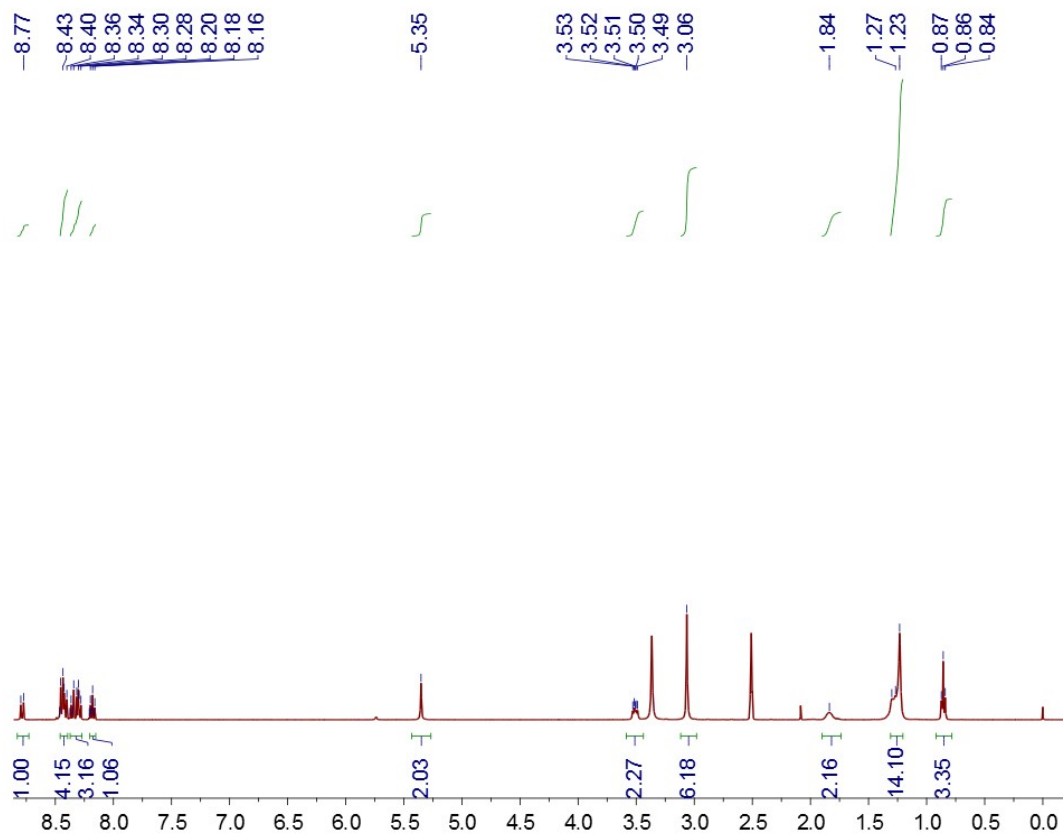


Fig. S4. ^1H NMR spectrum (500 MHz, $\text{DMSO-}d_6$, 293 K) of PyAC.

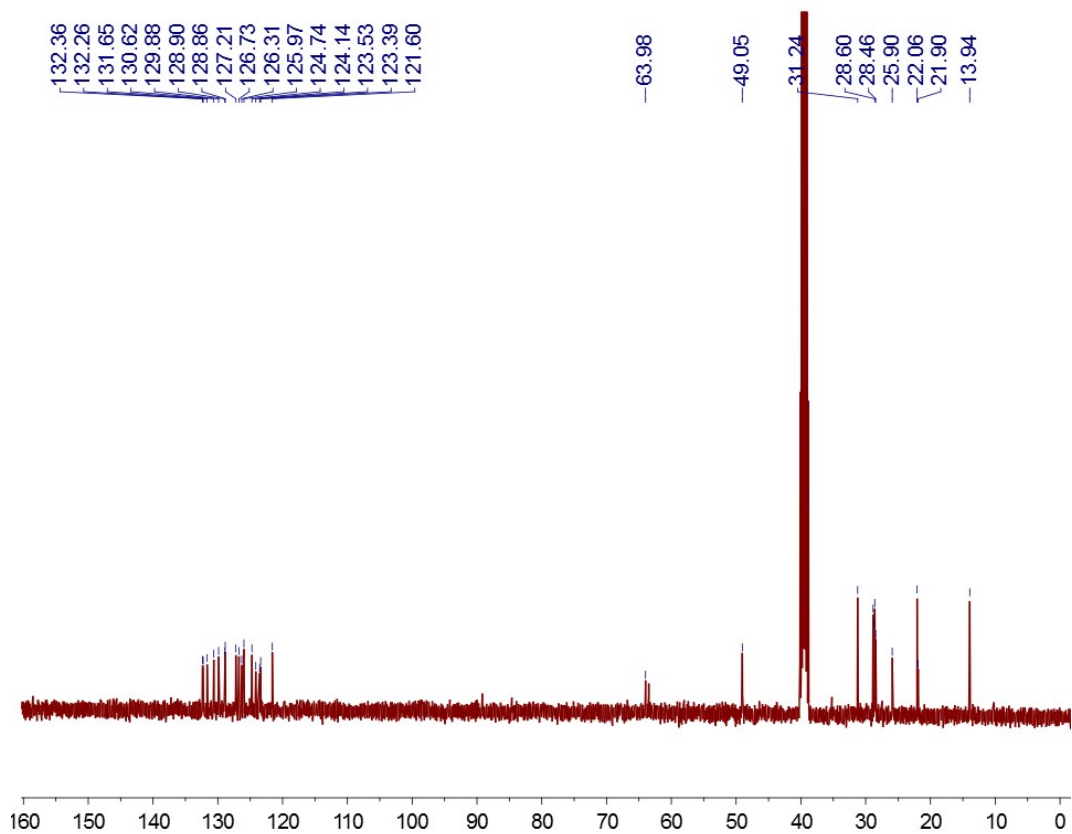


Fig. S5. ^{13}C NMR spectrum (125 MHz, $\text{DMSO-}d_6$, 293 K) of PyAC.

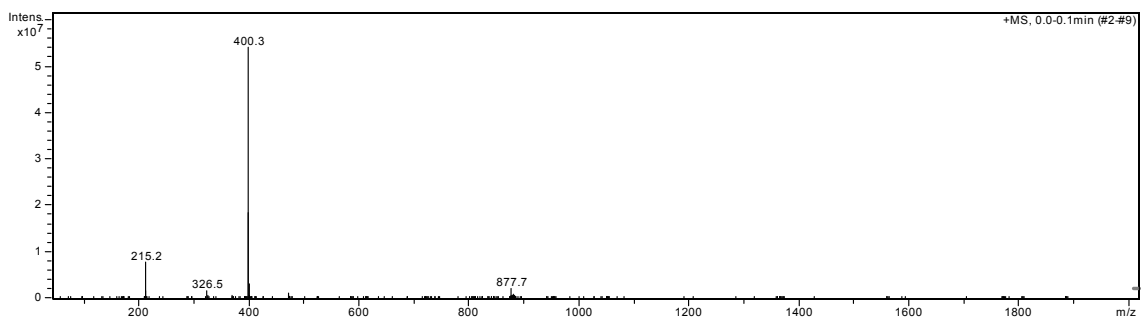


Fig. S6. Electrospray ionization mass spectrum of **PyAC**. Assignment of the main peak: m/z 400.3 $[M - Br]^+$ (100%).

3. 2D NOESY spectra of **WP10**↔**G**

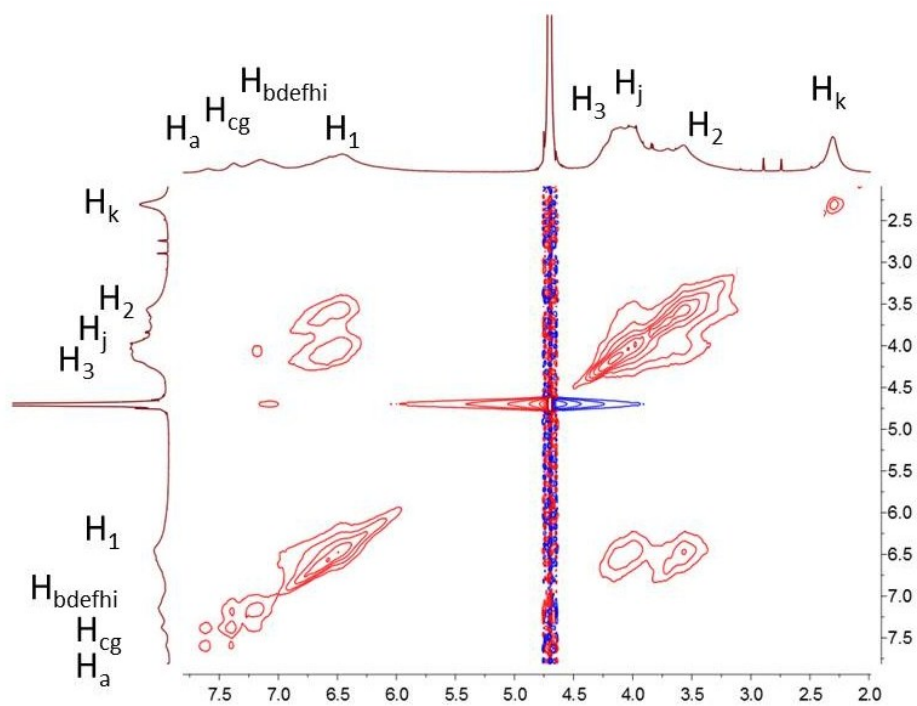
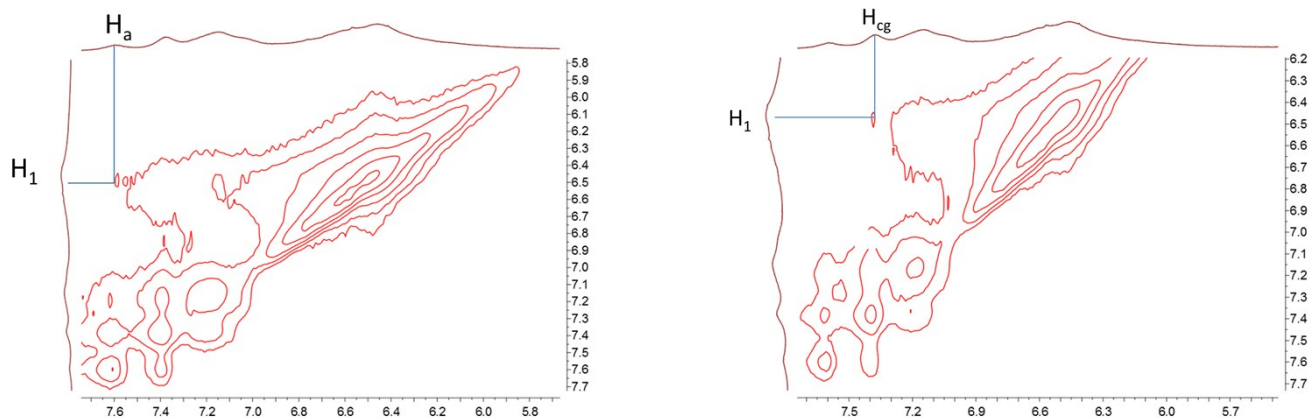


Fig. S7. 2D ^1H - ^1H NOESY spectrum of **WP10** (10.0 mM) and **G** (10.0 mM) (500 MHz, D_2O , room temperature).



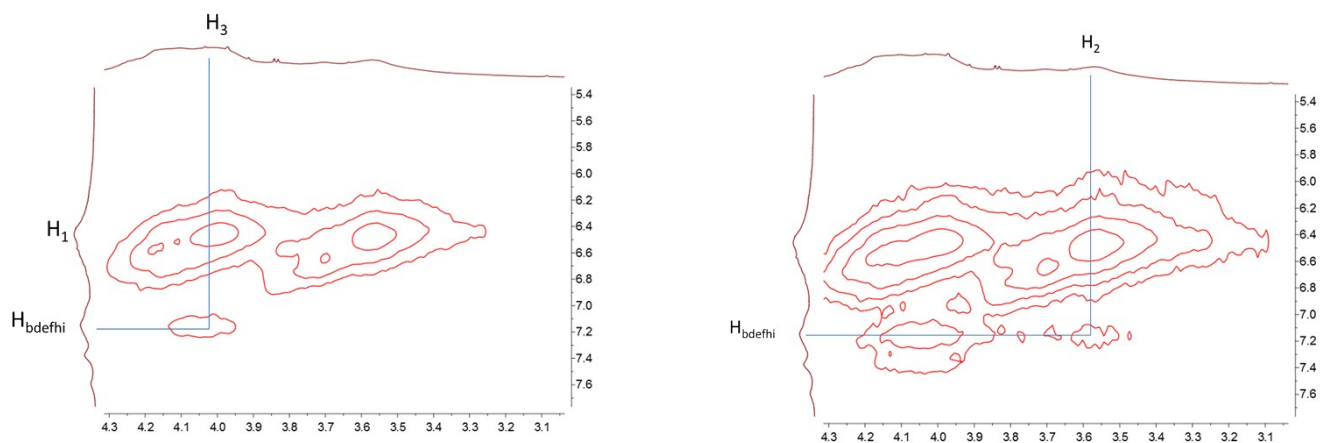


Fig. S8. Partial 2D ^1H - ^1H NOESY spectra of **WP10** (10.0 mM) and **G** (10.0 mM) (500 MHz, D_2O , room temperature).

4. Isothermal titration calorimetry (ITC) experiment

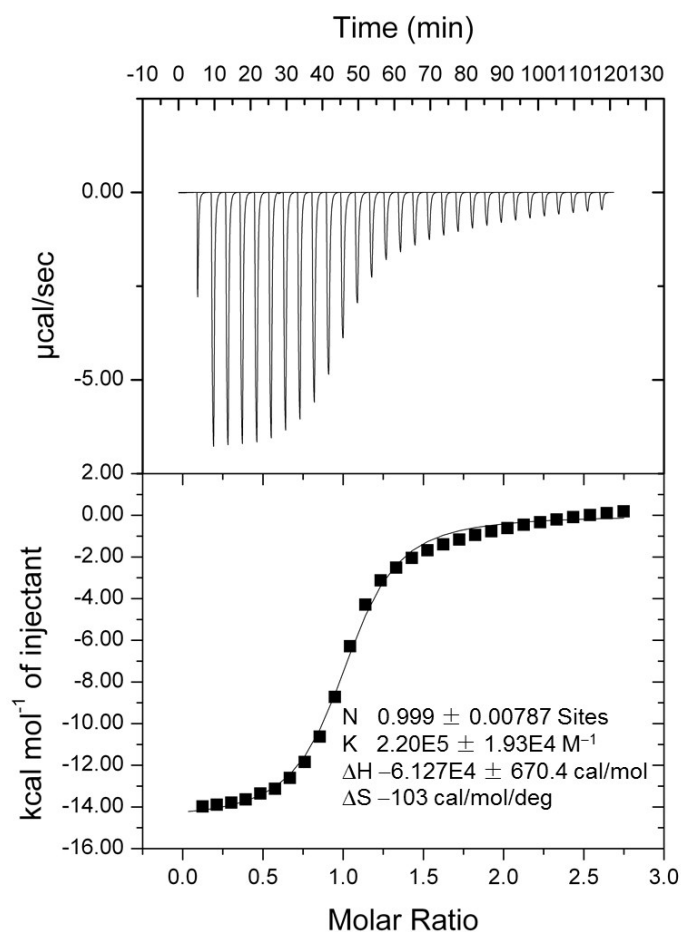


Fig. S9. Microcalorimetric titration of **G** with **WP10** in water at 298.15 K. Top: raw ITC data for 29 sequential injections (10 μL per injection) of a **G** solution (10.0 mM) into a **WP10** solution (0.50 mM); Bottom: net reaction heat obtained from the integration of the calorimetric traces.

Isothermal titration calorimetry (ITC) experiments were performed to provide thermodynamic insight into the inclusion complexation between **WP10** and **G**. As shown in Fig. S10, the K_a value of **WP10** \supset **G** was determined to be $(2.20 \pm 0.19) \times 10^5 \text{ M}^{-1}$ in 1:1 complexation. Furthermore, the enthalpy and entropy changes were obtained ($\Delta H^\circ < 0$; $T\Delta S^\circ < 0$; $|\Delta H^\circ| > |T\Delta S^\circ|$), indicating that this complexation was primarily driven by the enthalpy changes.

5. Critical aggregation concentration (CAC) determination of **PyAC** and **WP10** \supset **PyAC**

Some parameters such as the conductivity, osmotic pressure, fluorescence intensity and surface tension of the solution change sharply around the critical aggregation concentration. The dependence of the solution conductivity on the solution concentration is used to determine the critical aggregation concentration. Typically, the slope of the change in conductivity versus the concentration below CAC is steeper than the slope above the CAC. Therefore, the junction of the conductivity-concentration plot represents the CAC value. To measure the CAC value of **PyAC** (or **WP10**⊃**PyAC**), the conductivities of the solutions at different concentrations were determined. By plotting the conductivity versus the concentration, we estimated the CAC value of **PyAC** (or **WP10**⊃**PyAC**).

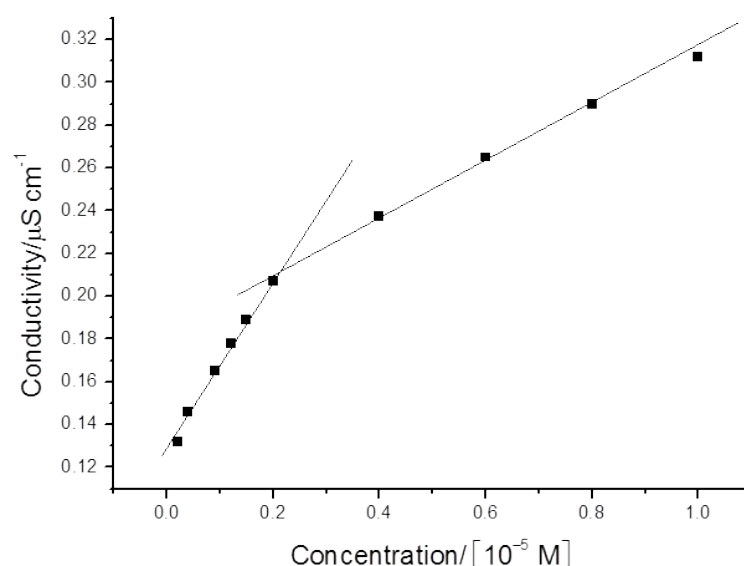


Fig. S10. The concentration-dependent conductivity of **PyAC**. The critical aggregation concentration (CAC) was determined to be 2.10×10^{-6} M.

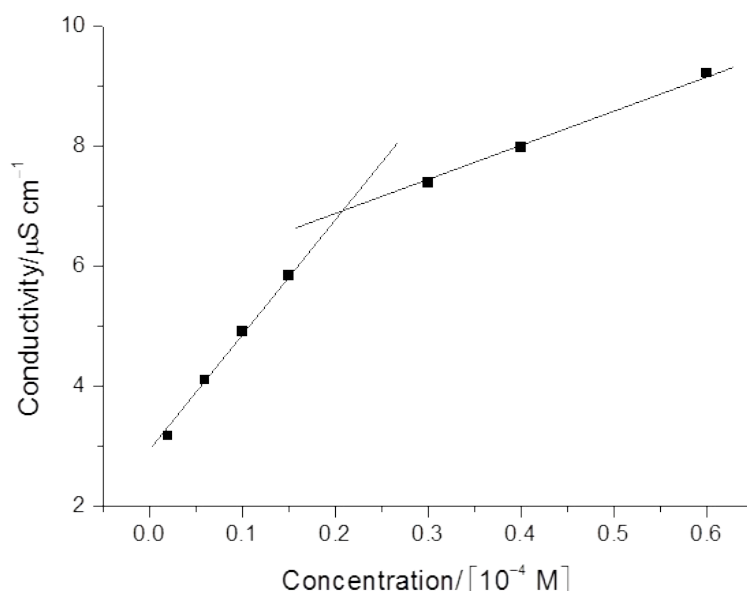


Fig. S11. The concentration-dependent conductivity of **WP10**⊃**PyAC**. The aqueous solutions used here are equimolar solutions of **WP10** and **PyAC** in water. The critical aggregation concentration (CAC) was determined to be 2.01×10^{-5} M.

6. DLS data of **WP10**⊃**PyAC**

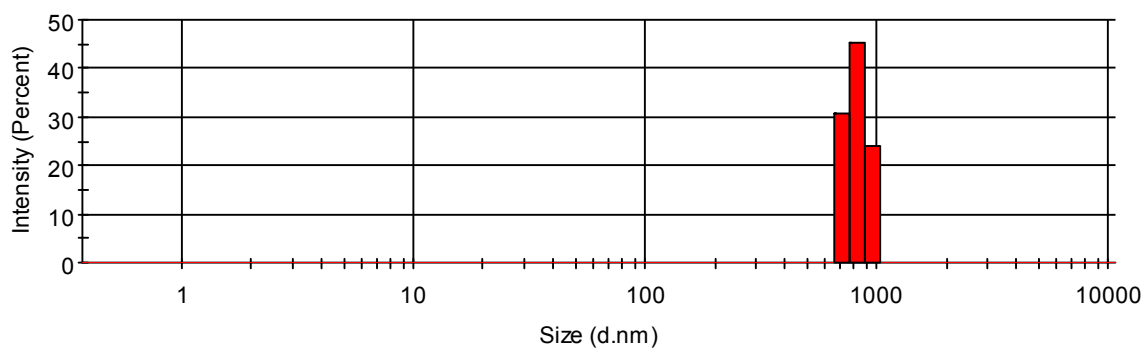


Fig. S12. DLS result of the vesicles formed by **WP10⊃PyAC**.

7. TEM images of G and WP10⊃G

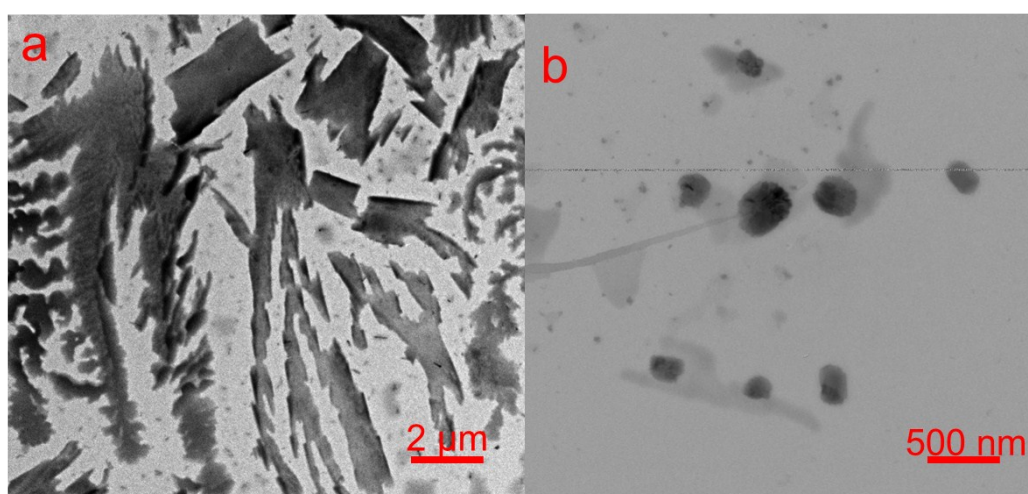


Fig. S13. TEM image of: (a) G, (b) **WP10⊃G**.

8. References:

- S1. A. Saha and S. Ramakrishnan, *Macromolecules*, 2009, **42**, 4028–403.
- S2. J. Yang, X. Chi, Z. Li, G. Yu, J. He, Z. Abliz and F. Huang, *Org. Chem. Front.*, 2014, **1**, 630-633.